High efficiency and nondissipative fast charging strategy

P.-H. Cheng and C.-L. Chen

Abstract: A high efficiency and nondissipative charging strategy for the fast battery charger is presented. The proposed charging strategy provides a charging method and an apparatus for rapidly charging the assembled batteries. The charging method has the advantages of high charging efficiency, rapid transient response and short charging time. Experimental verification is performed on 12 V/4.5 AH nonspillable sealed-lead assembled batteries.

1 Introduction

Recently, Portable electronic products have proliferated. The Battery is one of the most popular energy-storage devices for these products. There has been a great deal of interest in developing faster and more efficient methods for charging batteries for applications such as portable computers, mobile phones, aerospace systems, and electric vehicles as well as for household electrical equipment.

There are various methods for charging. Constant current charging does not change appreciably in magnitude, regardless of battery voltage or temperature. The battery is charged at a low charging rate. This charging scheme may prolong the charging time. In constant voltage charging, the initial charging current is normally high. The heating effect may damage the plate and shorten the life of the assembled batteries. Another charging method is called constant current/constant voltage charging. It is composed of two charging modes. In the initial charging, the battery chargers provide constant charging current until the terminal voltage increases up to a set value. Once it reaches the set voltage, the charging current decreases until the battery is completely charged. Therefore, voltage regulation is an important aspect of constant voltage charging.

To improve charging time and battery life of battery charges, several fast charging algorithms have been proposed and patented [1–3]. A better charging efficiency and a shorter charging time can be achieved by using the pulse-charge method [4–6]. A representative fast charging cycle is illustrated in Fig. 1. The charging scheme consists of a charging pulse immediately followed by a short and deep discharging pulse, and then a waiting period. The charging and discharging procedure is repeated until the assembled batteries are fully charged. To apply the technique and implement the current waveform of the pulse-charge method, a block diagram of a general fast charging circuit is shown in Fig. 2. The slopes of the rising and falling edges of charging pulses are bounded by the output filter inductance. A compromise between rapid transient response and low current ripple is quite difficult in power circuit design. In addition, using the discharging resistance to achieve a deep discharging pulse will lead to increased power consumption in the discharging period. Therefore, the major drawback of the pulse-charge method is poor efficiency in the charging circuit.

In this paper, a high efficiency and nondissipative fast charging strategy is presented. The fast charging circuit has a fixed switching frequency. It is always operated in the continuous conduction mode, and all power switches are zero voltage switched.

2 Nondissipative charging strategy

Fig. 3 shows the proposed nondissipative fast charging strategy. It consists of three operational modes: the active-charge mode, the active-discharge mode, and the inactive rest mode. During the active-charge mode, a series of charging triangular currents with a high DC component is applied. In the active-discharge mode, a series of sharp depolarisation triangular currents with much shorter duration is applied to pull the electrolytic ions away from

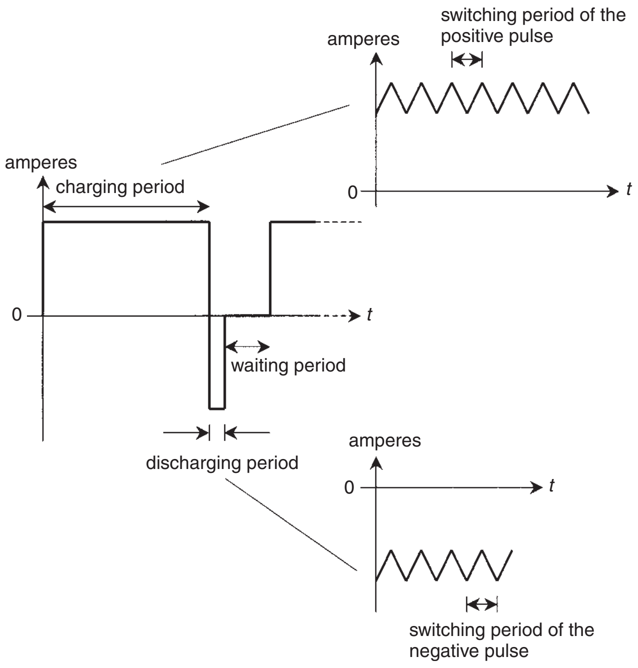

Fig. 1 *Representative fast charging cycle*

IEE Proceedings online no. 20030255
doi:10.1049/ip-epa:20030255
Paper first received 15th January 2002 and in revised form 10th December 2002. Originally published online: 19th June 2003

The authors are with the Department of Electrical Engineering, National Taiwan University, Room 546, Taipei 10617, Taiwan

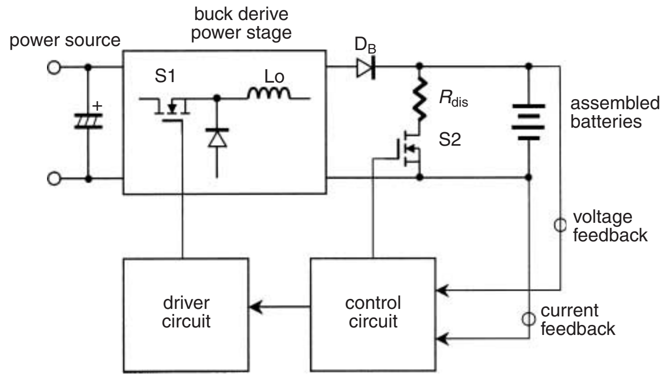

Fig. 2 *Block diagram of general fast battery charger*

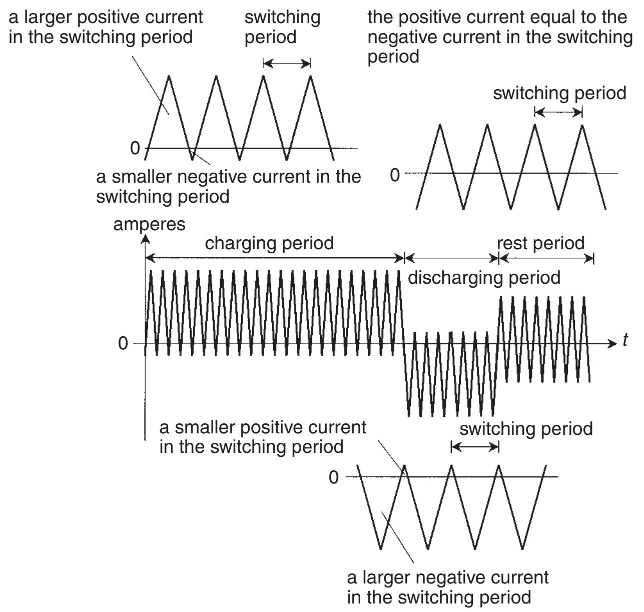

Fig. 3 *Proposed nondissipative fast charging strategy*

the plates. Finally, a stabilisation/rest period is used to position the ions at an appropriate distance from the plate surfaces; the amplitude of the positive current is equal to the negative current. The bipolar–triangle pattern is periodically repeated until a desired quantity of energy has been transferred into the assembled batteries.

3 Circuit description and operating analysis

The circuit diagram and some key waveforms of the proposed fast charging system are given in Fig. 4. It consists of two MOSFET switches (M1 and M2), connected as a synchronous rectifier buck configuration, input capacitor C_{in}, filtering inductor L_P and assembled batteries V_b. D1 and D2 are the anti-parallel body diodes of switches M1 and M2, respectively. C1 and C2 are the parasitic capacitors of switches M1 and M2, respectively. To avoid simultaneous conduction of M1 and M2, the dead time between the turn-off instant of switch M1 and the turn-on instant of the M2, as well as between the turn-on instant of switch M1 and the turn-off instant of the M2, must be introduced in the gate driver circuit of the two switches. The proposed fast charging circuit is a bidirectional power conversion that allows the power to be transferred between the power source and the assembled batteries in either direction. During the forward power flow mode, it is a buck converter and, during the reverse power flow mode, it is a boost converter. For both modes of operation, the battery voltage regulation is achieved by controlling the duty ratio of M1 and M2. Circuit operations in one complete switching period are described in detail below.

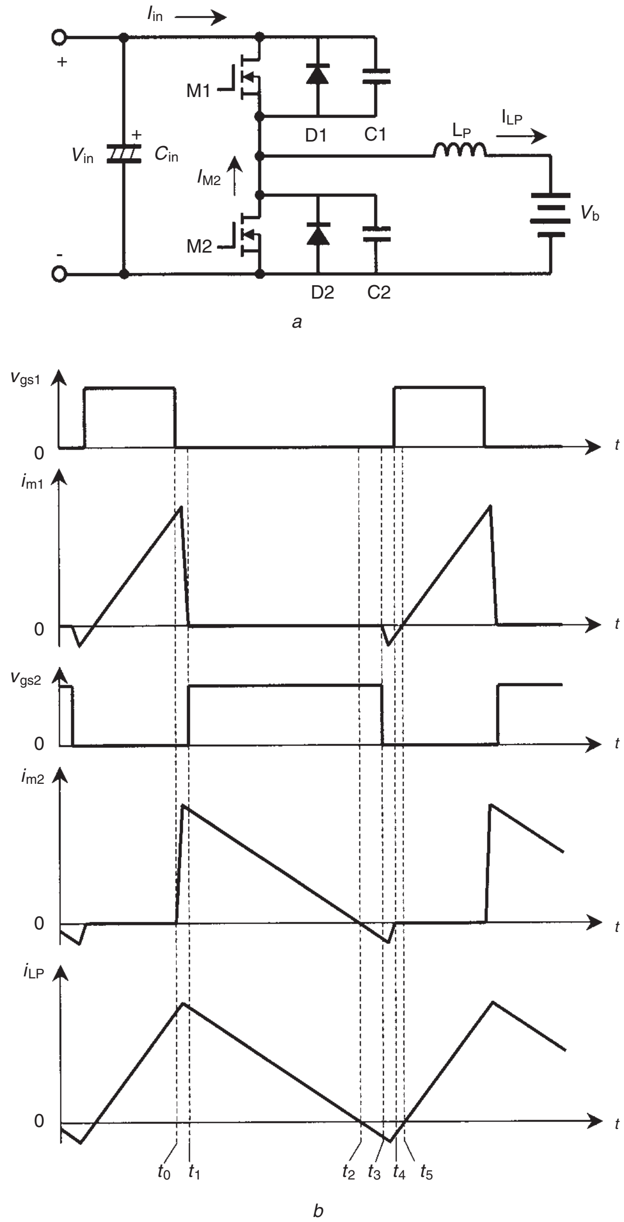

Fig. 4 *Circuit diagram and key waveforms of proposed fast charging system*

3.1 Forward power flow mode

The charging circuit for this mode of operation is shown in Fig. 5. The direction of power flow is from the power source

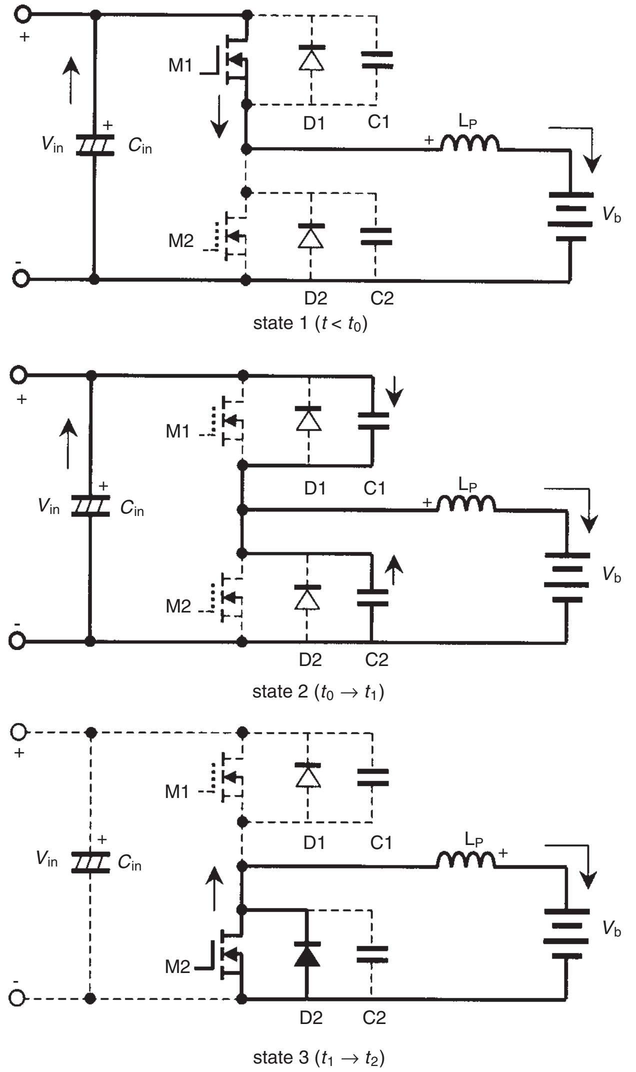

Fig. 5 *Forward power flow modes of proposed fast charging circuit*

to the assembled batteries, which are in charging mode. The circuit goes through the following four topological states within a half-switching cycle.

3.1.1 State 1 ($t<t_0$):

Just before t_0, switch M1 is on and the M2 is off, L_P is charged up linearly by the voltage V_{in}–V_b. The power source has transferred energy to the assembled batteries via L_P. The voltage across switch M2 is clamped at the input voltage V_{in}.

3.1.2 State 2 ($t_0 \rightarrow t_1$):

Two switches M1 and M2 are turned off at t_0, Capacitor C1, which is in parallel with M1, is charged up by the input current. Capacitor C2, which is in parallel with M2, is discharged. The voltage across switch M1 increases and the voltage across the switch M2 decreases. This state terminates at $t = t_1$ until the voltage across switch M_1 increases to the input voltage V_{in} and the voltage across the M_2 decreases to zero. L_P remains in charging mode.

3.1.3 State 3 ($t_1 \rightarrow t_2$):

At t_1, the voltage across the drain and source of M2 is reduced to zero, and the body diode of M2 starts conducting. The gate signal to M2 has been applied and the switch M2 is turned on under zero-voltage condition. The voltage across M1 is clamped at the input voltage V_{in}. The voltage across L_P is V_b so that the current in L_P begins to decrease linearly with slope V_b/L_P. L_P is now discharging.

3.2 Reverse power flow mode

The discharging circuit for this mode of operation is shown in Fig. 6. The direction of power flow is from the assembled batteries to the power source. The assembled batteries are discharging. The circuit goes through the following four topological states within a half-switching cycle.

3.2.1 State 4 ($t_2 \rightarrow t_3$):

At t_2, switch M2 is kept on. The current in L_P decreases to zero and then changes polarity. At this time, the assembled batteries charge L_P and the current in L_P starts increasing.

3.2.2 State 5 ($t_3 \rightarrow t_4$):

At t_3, switch M2 is turned off. C2 starts to be charged by the discharging current of the assembled batteries. The voltage across M1 decreases. This state terminates at $t = t_4$ until the voltage across M2 increases to the input voltage V_{in} and the voltage across the

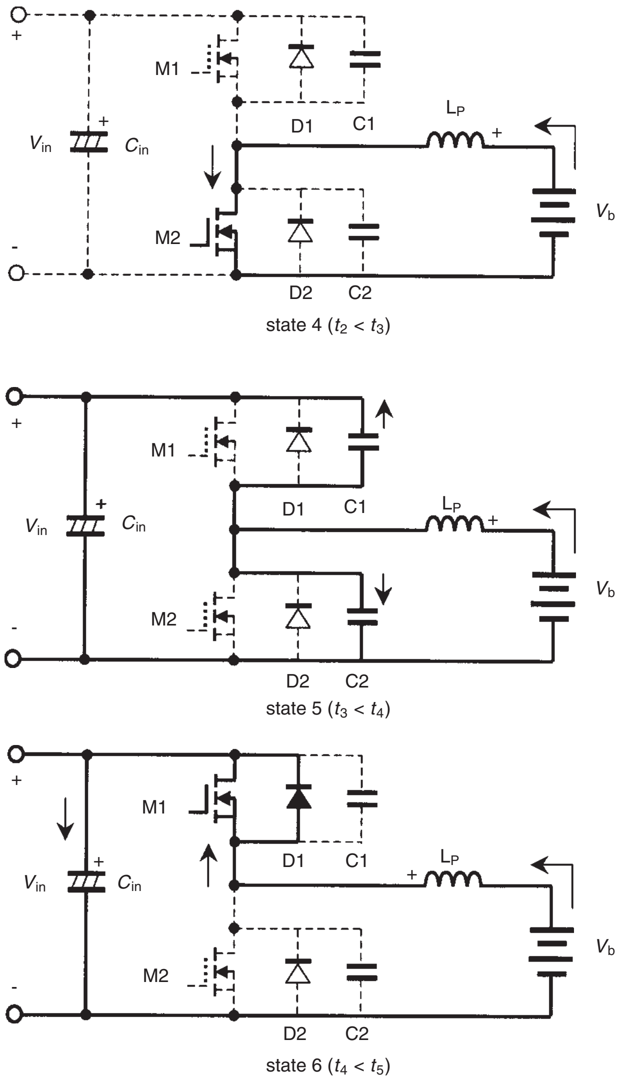

Fig. 6 *Reverse power flow modes of proposed fast charging circuit*

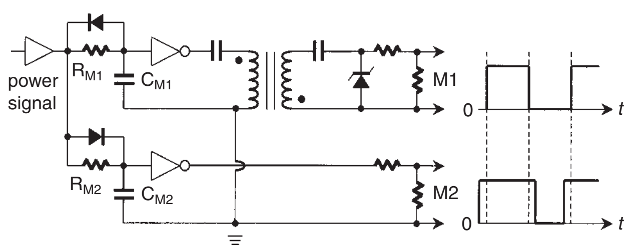

Fig. 7 *Gate drive circuit of two switches*

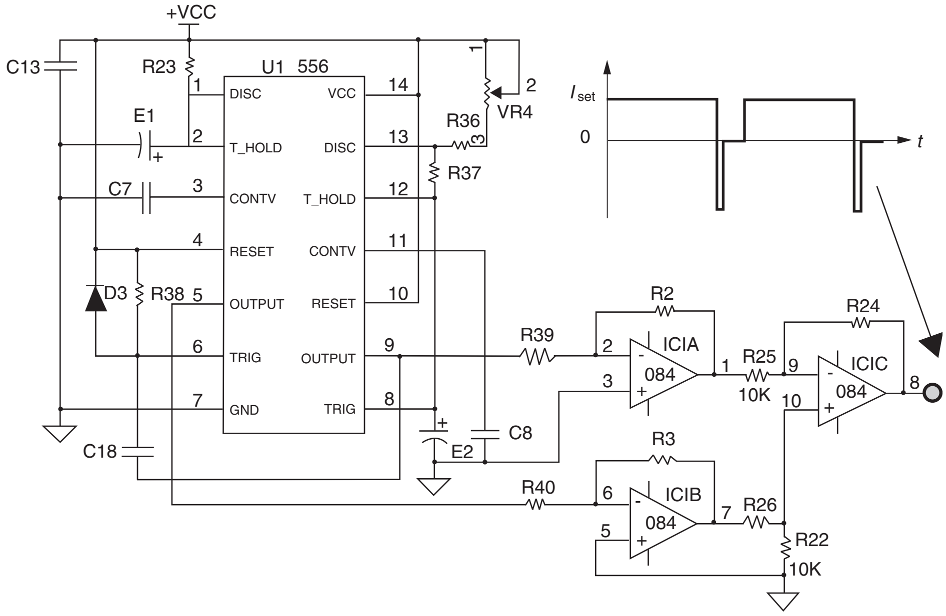

Fig. 8 *Setting current circuit of proposed fast charger*

drain and source of M1 is zero. L_P remains in charging mode and the current in L_P continues to increase.

3.2.3 State 6 ($t_4 \rightarrow t_5$):

At t_4, the voltage across the drain and source of M1 is zero, and the body diode of M1 conducts. The gate signal to M1 has been applied and the switch M1 is turned on under zero-voltage condition. The voltage across M2 is clamped at the input voltage V_{in}. The voltage across L_P is V_{in}–V_b so the current in L_P begins to decrease and L_P is discharging. The battery discharging current decreases linearly. While the current in L_P decreases to zero and then changes polarity, switch M1 keeps conducting. The power source transmits energy to the assembled batteries.

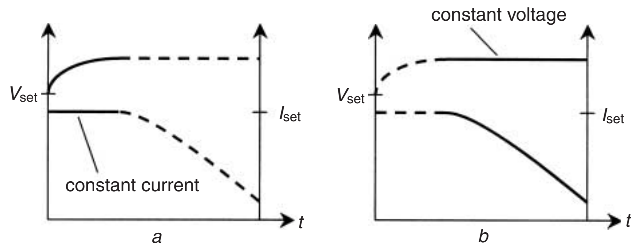

Fig. 9 *Primary charging modes of operations*
a with constant current mode
b with constant voltage mode

4 Design and implementatation

4.1 Gate drive

The control signals of the two switches M1 and M2 are obtained by using a current mode PWM control IC, UC3845. The switching frequency is 40 kHz. The gate drive to switch M2 is the inversion of the gate drive to M1, with a small dead time in-between the turn-off of one switch and the turn-on of the other. Fig. 7 shows a gate drive circuit of the two switches.

4.2 Input capacitor

During the discharging period, the assembled batteries must transfer the stored energy to the power source. This should absorb the discharging energy, and a few larger capacities in an electrolytic capacitor are used. The input capacitor can be obtained from the following equation:

$$C_{in} = \frac{I_{dis} \cdot t_{dis}}{\Delta V_{in}} \qquad (1)$$

where ΔV_{in} is the ripple voltage in the input terminal, t_{dts} is the discharging time and I_{dts} is the discharging current from the assembled batteries.

4.3 Current reference

The setting current circuit of the proposed fast charger is shown in Fig. 8. To obtain the depolarisation current, we make the setting current negative. Three current commands in the charging period, discharging period and rest period are achieved by using a dual output timer, IC556.

4.4 Charging modes

Fig. 9 shows the primary charging modes of operations in the proposed fast charging circuit: constant current mode and constant voltage mode. In the constant current mode, feedback voltage V_{fb} is smaller than setting voltage V_{set}, the error voltage V_{err} is too large so that the voltage controller is in disabled mode and therefore the battery voltage increases linearly to the desired value. The feedback current is very close to the setting current I_{set} and therefore the error current I_{err} is small, the current controller is the dominant action. At the same time, the charging current is regulated to the preset value. In constant voltage mode, the voltage in feedback is very close to the setting voltage V_{set} and therefore the error voltage V_{err} is small. The battery voltage is a constant value. The feedback current I_{fb} is smaller than the setting current I_{set} and the error current I_{err} is large, so the charging current decreases linearly to the desired value. Because there are two controllers in the charging circuit, we have to disable the error amplifier in control IC and add an additional operational amplifier in the control loop. A block diagram of the voltage and current controller is shown in Fig. 10.

4.5 Calculation of the charging efficiency

To calculate the charging efficiency, we have to record the charging and discharging capacity. The charging efficiency

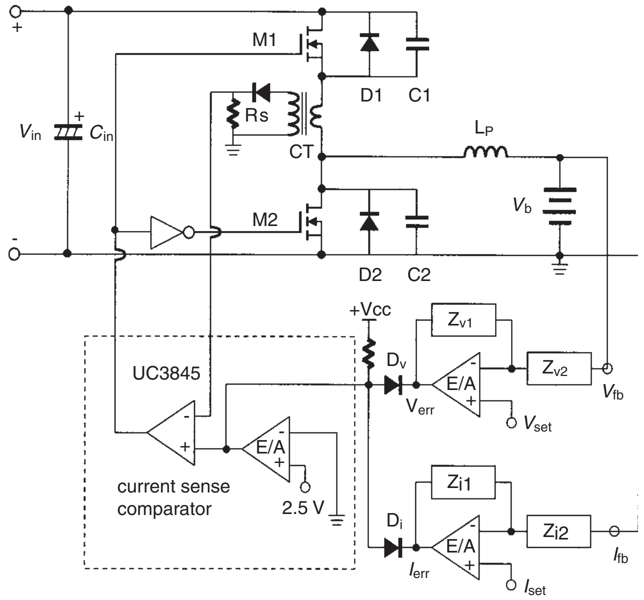

Fig. 10 *Block diagram of voltage and current controller*

Table 1: List of the parameters of the fast charging system

Assembled batteries	12 V–4.5 AH Nonspillable sealed-lead rechargeable battery Total six units in serial connection
Power switches	MOSFET, IRFP260, 200 V, 46 A, 55 mΩ
PWM control 1C	UC3845
Switching frequency	40 kHz
Filter inductor	5.5 μH, 4 T, Kool Mu 77442-A7
DC bus capacitor	1980 μF
DC bus voltage	48 V
Setting voltage	14.6 V
Charging current	16 A maximum
Output power	240 W maximum

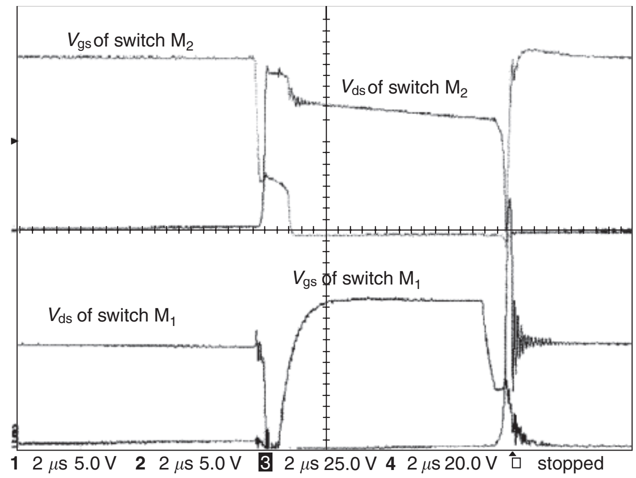

Fig. 11 V_{ds} *and* V_{gs} *waveforms of switches M1 and M2*

is written as:

$$\eta\% = \frac{\int_{t_{d0}}^{t_{dn}} i_d(t) \cdot dt}{\int_{t_{c0}}^{t_{cn}} i_c(t) \cdot dt} \tag{2}$$

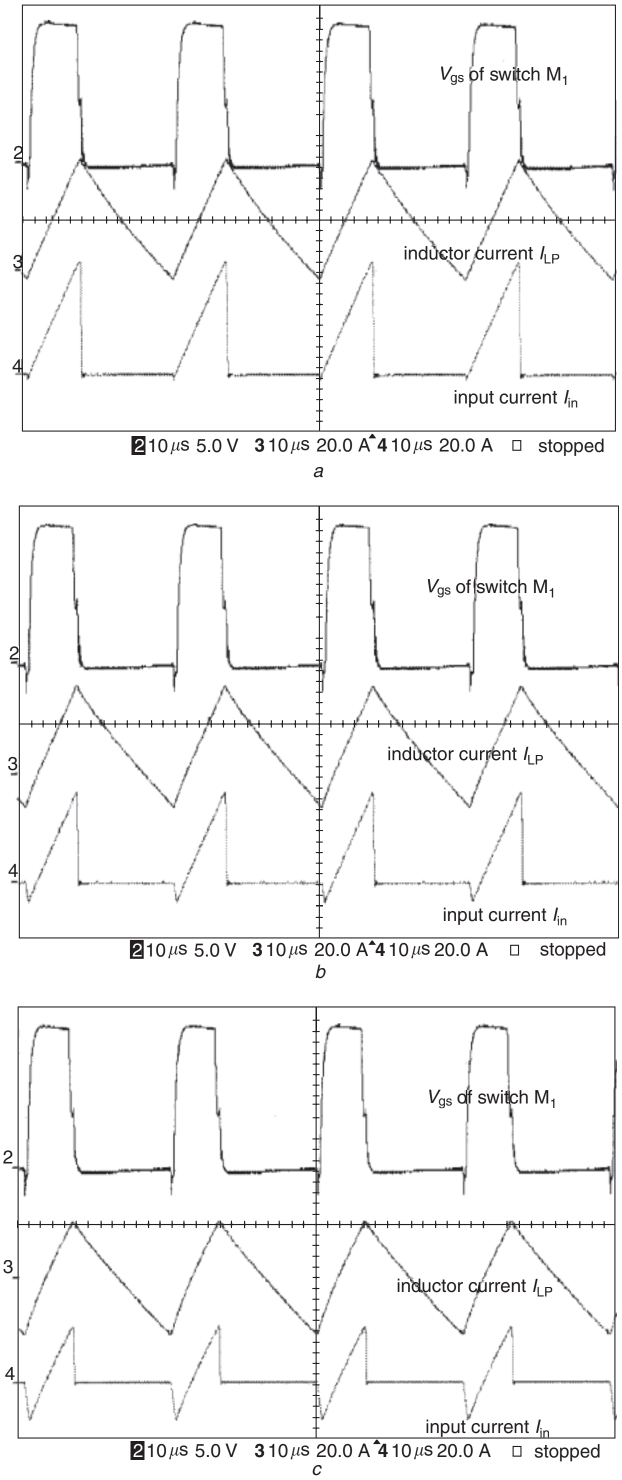

Fig. 12 *Measured waveforms of proposed fast charger with different charging status*
a with constant current mode at full load ($V_b = 13.8$ V, $I_O = 16$ A)
b with constant voltage mode at half load ($V_{bavg} = 14.6$ V, $I_{LPavg} = 8$ A)
c with constant voltage mode at light load ($V_{bavg} = 14.6$ V, $I_{LPavg} = 1.0$ A)

where $i_c(t)$ is the charging current and $i_d(t)$ is the discharging current. t_{c0} is the initial time and t_{cn} is the final time for the charging status. t_{d0} is the initial time and t_{dn} is the final time for the discharging status.

5 Experimental verification

To experimentally characterise the nondissipative charging strategy and a charging circuit for the fast battery charger, a

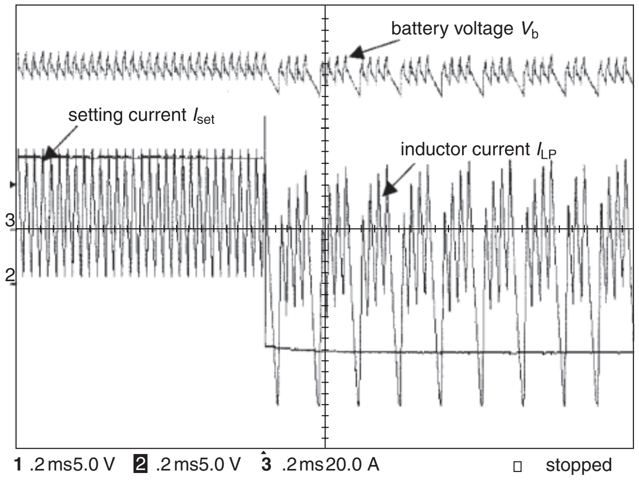

Fig. 13 *Experimental waveforms of proposed circuit in transition state*

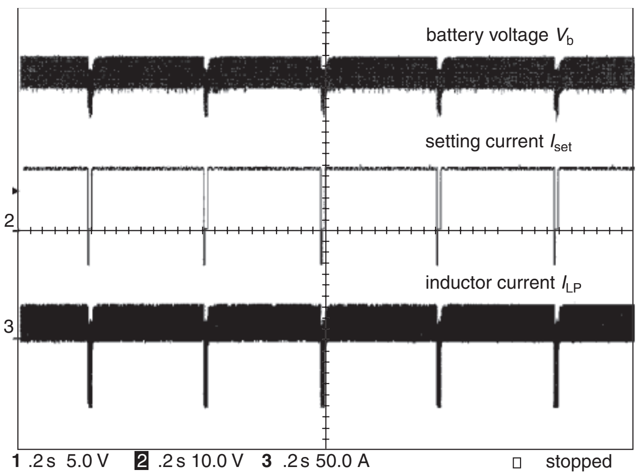

Fig. 14 *Experimental waveforms of proposed circuit in constant current mode*

fast charging system was constructed to the specifications listed in Table 1. Fig. 11 shows the voltage across the drains and sources of M1 and M2, the voltage across the gates and the sources of M1 and M2. The experimental results exhibit the zero-voltage state in the switches and the bipolar–triangle current waveform is implemented by using the proposed circuit. The current in L_P and the input current of the fast charging circuit with constant current mode at full load ($V_O = 13.8$ V and $I_O = 16$ A) are shown in Fig. 12(*a*), with constant voltage mode at half-load ($V_O = 14.6$ V, and $I_O = 8$ A) are shown in Fig. 12(*b*), and with constant voltage at light load ($V_O = 14.6$ V, and $I_O = 1.0$ A) are shown in Fig. 12(*c*). There is an apparent discharging current transferred the stored energy from the assembled batteries to the power source in the input current waveforms. The experimental waveforms in Fig. 13 show the battery voltage, the setting current and the current in L_P in the transition state. While the charging period is changing to the discharging period, the current in L_P is in rapid transition by transformation of the setting current. It is noted that the charging current is always greater than the discharging current during the charging period, and the discharging current is always larger than the charging current during the discharging period. Fig. 14 shows the experimental waveforms of the proposed circuit in the constant current mode. It includes a few charging and discharging periods. Fig. 15 shows the charging process of

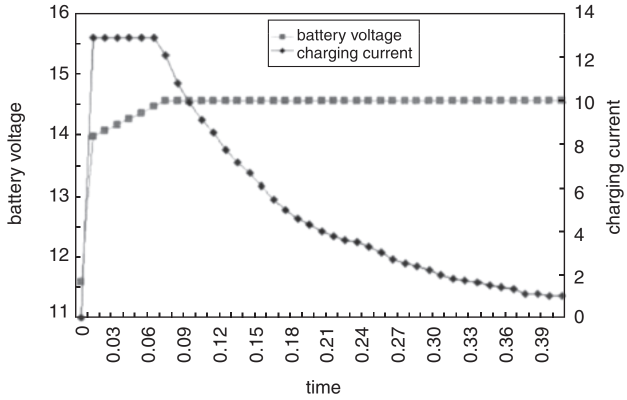

Fig. 15 *Charging process of proposed fast charger*

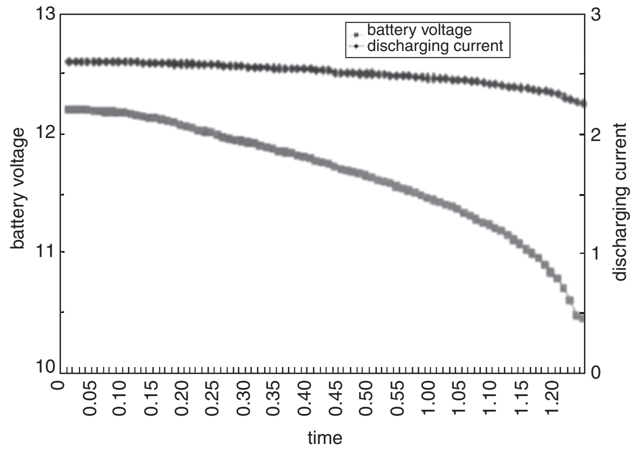

Fig. 16 *Discharging process of assembled batteries*

the proposed fast charger. Fig. 16 depicts the discharging process of the assembled batteries. In the experiment, the charging capacity is 3.71 AH in 40 minutes and the discharging capacity is 3.5 AH in 90 minutes. Therefore, the charging efficiency is about 94.3%. In addition, the charging time is no more than 10 minutes from empty to 50% of full charge and no more than 30 minutes from empty to 80% of full charge.

6 Conclusions

Low efficiency is unavoidable in the pulse-charge fast charging method, due to resistive discharging. In this paper, a high efficiency and nondissipative charging strategy for the fast battery charger is proposed. All power switches are operated with zero-voltage switching. The charging strategy and charging circuit presented are experimentally verified on 12 V/4.5 AH nonspillable sealed-lead assembled batteries. The charging efficiency reaches 94.3%, the charging time is no more than 10 minutes from empty to 50% of full charge and no more than 30 minutes from empty to 80% of full charge.

7 References

1 Valeriote, E.M., Chang, T.G., and Jochim, D.M.: 'Fast charging of lead–acid batteries'. Proceedings of the Battery Conference on Applications and advances, 11–13 January 1994, pp. 33–38

2 Freeman, D., and Heacock, D.: 'Advanced charger designs address modern battery technologies'. Proceedings of WESCON'93, 28–30 September 1993, pp. 226–231

3 Hung, S.T., Hopkins, D.C., and Mosling, C. R.: 'Extension of battery life via charge equalization control', *IEEE Trans. Ind. Electron.*, 1993, **40**, pp. 96–104
4 Martin, L.J., and Garrett, S.M.: 'Method of rapidly charging a lithium ion cell'. US patent, 5 481 174, 1996
5 Podrazhansky, Y., and Popp, P.W.: 'Rapid battery charger, discharger and conditioner' US patent, 4 829 225, 1989
6 Podrazhansky, Y., and Popp, P.W.: 'Method and apparatus for charging, thawing, and formatting a battery' US patent, 5 307 000, 1994